Inorg. Chem. **2002**, *41*, 1782–1787

Pairwise Exchanges of Oxo and Imido Groups in Rhenium(VII) Compounds

Wei-Dong Wang* and James H. Espenson*

Contribution from the Ames Laboratory and the Department of Chemistry, Iowa State University, Ames, Iowa 50011

Received October 15, 2001

The kinetic and thermodynamic parameters for the oxo and imido exchange reactions among $MeReO_3$, $MeReO_2(NR)$, $MeReO(NR)_2$, and $MeRe(NR)_3$ (R = 1-adamantyl, Ad; or 2,6-diisopropylphenyl, Ar) have been measured. The rate constant for the NAr series decreases from 0.27 to 0.0024 L mol^{-1} s^{-1} at 25 °C in benzene as the total number of participating imido groups increases from 2 to 4, indicating that steric effects play an important role in the kinetics of the ligand exchange reactions. But, with NAd, the values of k/L mol^{-1} s^{-1} are 0.2 (4 NAd), 100 (3 NAd), and 0.74 (2 NAd). The equilibrium constants, also subject to steric effects, are much larger than those predicted by ligand combination statistics and greatly favor the mixed oxo–imido compounds. The different steric demands by imido and oxo ligands are believed to be the main factor for the larger equilibrium constants because the equilibrium constant shows minimal dependence on temperature. The large negative activation entropies for the ligand exchange reactions are consistent with a metathesis mechanism featuring nearly concurrent interchange of oxo and imido groups.

Introduction

The compounds $MeRe(NR)_3$ (R = Ad = 1-adamantyl;[1,2] R = Ar = 2,6-diisopropylphenyl[3]) are isoelectronic and isostructural analogues of the better known $MeReO_3$ (MTO).[4] Both $MeRe(NAd)_3$ and $MeRe(NAr)_3$ are monomeric in the solid state as well as in solution. The mixed-ligand compounds $MeReO(NR)_2$ and $MeReO_2(NR)$ are also known, and the arylimido series have been structurally characterized: when crystalline, they exist as (μ-O)$_2$ dimers but are predominantly monomeric in solution at room temperature.[3] Their structural formulas in solution are given in Chart 1; we use the notation (***m***,***n***) to designate the species $MeReO_m(NR)_n$, with **a** for R = NAd and **b** for R = NAr.

Since the discovery of alkene metathesis,[5,6] metathetical reactions have been extended to alkynes[7−10] and imines.[11−13] Metathesis between two metal ligand multiple bonds, eq 1, although known, has been less well studied.[11,14]

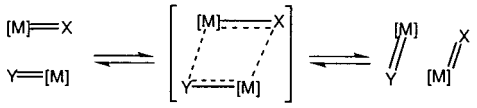

(1)

Exchange reactions between arylimido- and oxo-rhenium(VII) complexes have been studied by Herrmann and coworkers. These processes take place through dimeric intermediates with bridging ligands. The decrease of reactivity of $MeRe(NAr)_3$ (**0**,**3b**), compared to $MeReO(NAr)_2$ (**1**,**2b**), toward $MeReO_3$ (**3**,**0**) is suggested because of the steric bulk

* Authors to whom correspondence should be addressed. E-mail: wangw@ameslab.gov (W.-D.W.); espenson@iastate.edu (J.H.E.).

(1) Wang, W.-D.; Espenson, J. H. *Organometallics* **1999**, *18*, 5170.
(2) Wang, W.-D.; Guzei, I. A.; Espenson, J. H. *Inorg. Chem.* **2000**, *39*, 4107.
(3) Herrmann, W. A.; Ding, H.; Kühn, F. E.; Scherer, W. *Organometallics* **1998**, *17*, 2751.
(4) Romão, C. C.; Kühn, F. E.; Herrmann, W. A. *Chem. Rev.* **1997**, *97*, 3197.
(5) Truett, W. L.; Johnson, D. R.; Robinson, I. M.; Montague, B. A. *J. Am. Chem. Soc.* **1960**, *82*, 2337.
(6) Natta, G.; Dall'Asta, G.; Mazzanti, G. *Angew. Chem., Int. Ed. Engl.* **1964**, *3*, 723.
(7) Wengrovius, J. H.; Sancho, J.; Schrock, R. R. *J. Am. Chem. Soc.* **1981**, *103*, 3932.
(8) Dias, E. L.; Grubbs, R. H. *Organometallics* **1998**, *17*, 2758.
(9) Brizius, G.; Pschirer, N. G.; Steffen, W.; Stitzer, K.; zur Loye, H.-C.; Bunz, U. H. F. *J. Am. Chem. Soc.* **2000**, *122*, 12435.
(10) Fürstner, A.; Grela, K.; Mathes, C.; Lehmann, C. W. *J. Am. Chem. Soc.* **2000**, *122*, 11799.
(11) Cantrell, G. K.; Meyer, T. Y. *J. Am. Chem. Soc.* **1998**, *120*, 8035.
(12) Zuckerman, R. L.; Krska, S. W.; Bergman, R. G. *J. Am. Chem. Soc.* **2000**, *122*, 751.
(13) Bruno, J. W.; Li, X. J. *Organometallics* **2000**, *19*, 4672.
(14) Jolly, M.; Mitchell, J. P.; Gibson, V. C. *J. Chem. Soc., Dalton Trans.* **1992**, 1331.

10.1021/ic011070p CCC: $22.00
Published on Web 03/05/2002

Chart 1. Structural Formulas of Oxo and Imido Rhenium(VII) Compounds

$MeRe(NR)_3$ (**0,3**) $MeReO(NR)_2$ (**1,2**) $MeRe(O)_2(NR)$ (**2,1**) $MeReO_3$ (**3,0**)

(**a**, R = Ad; **b,** R = Ar) (**a**, R = Ad; **b,** R = Ar) (**a**, R = Ad; **b,** R = Ar)

of the arylimido ligand.[3] There are three imido/oxo exchange reactions of rhenium(VII) complexes that will lead to net observable chemical change, as follows:

$$MeReO_3 + MeRe(NR)_3 \rightleftarrows MeReO_2(NR) + MeReO(NR)_2 \quad (2)$$

$$MeReO_2(NR) + MeRe(NR)_3 \rightleftarrows 2MeReO(NR)_2 \quad (3)$$

$$MeReO_3 + MeReO(NR)_2 \rightleftarrows 2MeReO_2(NR) \quad (4)$$

Only two of three have independent thermodynamics and kinetics, owing to these requirements:

$$K_2 = K_3 \times K_4; \frac{k_2}{k_{-2}} = \frac{k_3}{k_{-3}} \times \frac{k_4}{k_{-4}} \quad (5)$$

Exchange is accomplished by the interchange of two ligands, concurrently or nearly so. Net chemical exchange occurs only when one oxo and one imido group are bridging.

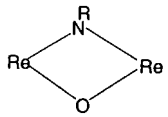

Otherwise, group exchange does not lead to net change and requires isotopic labeling for its characterization. The latter are delineated in the Supporting Information but are not presented here because most of our data do not bear directly on them.

We have used NMR methods to determine the equilibrium constants for the three reactions given. We have also evaluated all six rate constants, some directly with NMR and spectrophotometric techniques, others by combining equilibrium and rate constants or by kinetic simulations. In the course of these studies, it became clear that ligand combination statistics was unable to account for the relative values of K and k; we have sought to define the various electronic and steric factors that enter the picture.

Experimental Section

Instruments and Reagents. A Bruker DRX-400 spectrometer was used to measure the ^{1}H NMR spectra, NMR kinetics, and equilibrium constants. A Bruker AC-200 spectrometer was used to record ^{17}O NMR spectra. A Shimadzu UV 3101PC spectrophotometer was used to study most of the exchange kinetics. Benzene (Aldrich) and benzene-d_6 (CIL) were dried with sodium/benzophenone and stored in a nitrogen-filled glovebox. Literature procedures were used to prepare $MeRe(NAd)_3$ (**0,3a**),[1] $MeReO_3$ (**3,0**),[15] $MeReO(NAr)_2$ (**0,2b**),[3] and $MeRe(O)_2(NAr)_2$ (**2,1b**).[3] The labeled compound $MeRe^{17}O_3$ was prepared by allowing $MeRe^{16}O_3$ to equilibrate in 20% $H_2{}^{17}O$ at room temperature for 8 h. The rhenium compound was then extracted into dichloromethane and isolated after solvent was removed. The use of ^{17}O NMR spectroscopy established the incorporation of ^{17}O into MTO.

Table 1. Equilibrium and Rate Constants for Oxo−Imido Exchange between Re(VII) Compounds

reaction	K_{298}	$k_{f,298}$/L mol^{-1} s^{-1}	$k_{r,298}$/L mol^{-1} s^{-1}
		R = Ad	
2	$1.0(1) \times 10^5$	$\sim 10^2$	$\sim 10^{-3}$
3	$3.7(3) \times 10^2$	~ 0.2	$\sim 5 \times 10^{-4}$
4	$2.60(25) \times 10^2$	$7.4(3) \times 10^{-1}$	$2.8(3) \times 10^{-3}$
		R = Ar	
2	$1.8(2) \times 10^3$	$1.7(1) \times 10^{-2}$	$9(1) \times 10^{-6}$
3	$2.2(2) \times 10^1$	$\sim 2.4 \times 10^{-3}$	$\sim 10^{-4}$
4	$8.4(7) \times 10^1$	$2.7(1) \times 10^{-1}$	$3.0(3) \times 10^{-3}$
5[b]	0.92	3.4×10^{-7} [a]	

Equilibrium Measurements. Because the proton resonances of C$\boldsymbol{H}_3$−Re in (**3,0**), (**2,1**), (**1,2**), and (**0,3**) are well separated,[2,3] ^{1}H NMR spectroscopy was used to measure the equilibrium constants at 298 K in C_6D_6. To ensure that equilibrium had been reached, measurements were made on solutions prepared with different initial concentrations. Data collection began 16 h after the initial solution was prepared and then repeated every 4 h until the calculated equilibrium constants were invariant. For certain experiments, the equilibrium constants were rechecked after a week. The initial conditions were altered by introducing either (**3,0**) or (**0,3**) into a solution of (**1,2**) or (**2,1**). The equilibrium constants in Table 1 did not change when the relaxation time was set at 1, 5, or 10 s and were averages of at least three measurements at different conditions. Tables S1−3 (in the Supporting Information) show the equilibrium concentrations of rhenium species and the equilibrium constant for individual runs.

Kinetics. Stock solutions of (**3,0**) and (**0,3**) in benzene were prepared and stored in a nitrogen-filled glovebox. Other stock solutions were prepared and used within 24 h. The electronic spectra of the adamantyl and aryl series are given in Figure 1. The kinetics of reactions 2−4 were studied by monitoring the absorbance changes at an appropriate wavelength or by following the intensity changes in the ^{1}H NMR spectra, maintaining an anaerobic environment. The temperature was controlled thermoelectrically in the range 10−40 °C.

(a) Reaction 4a. When (**3,0**) and (**0,3a**) were used, with the former in substantial stoichiometric excess, the first step occurred so rapidly that the principal components were then (**3,0**) and (**1,2a**); reaction 3a is precluded since [(**0,3a**)] is nearly zero. At that point, reaction 4a could then be monitored. Given the excess concentration of (**3,0**) and the favorable equilibrium constant, $K_{4a} = 2.6 \times 10^2$,

(15) Herrmann, W. A.; Kratzer, R. M.; Fischer, R. W. *Angew. Chem., Int. Ed. Engl.* **1997**, *36*, 2652.

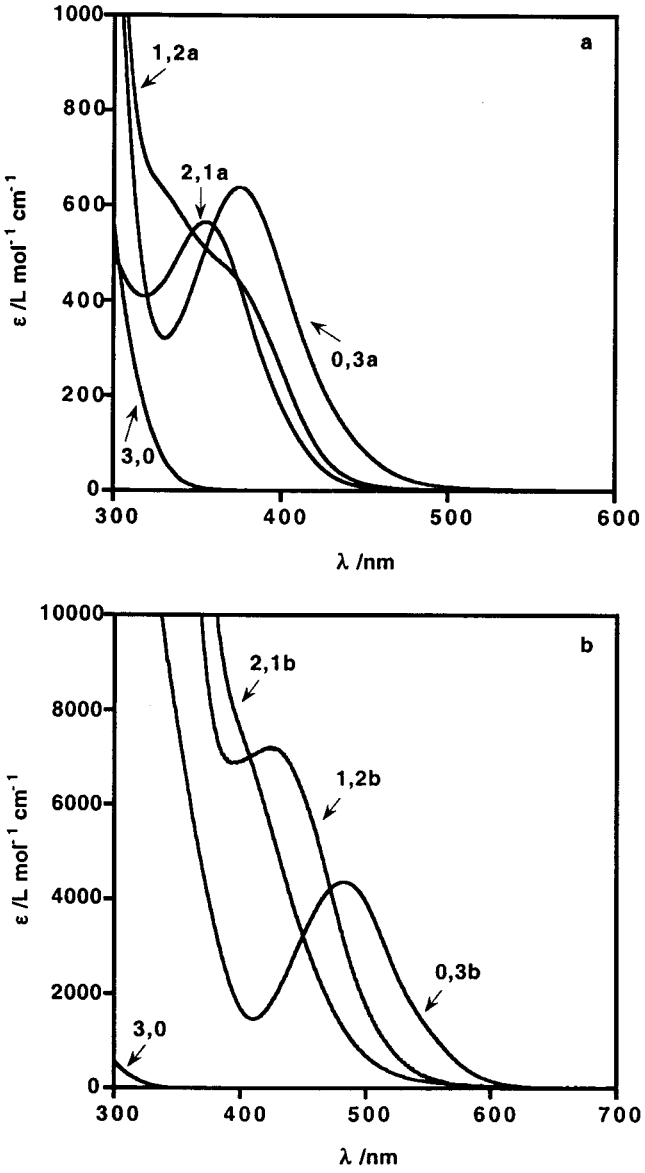

Figure 1. (a) Electronic spectra of $MeReO_m(NAd)_n$ (Ad = 1-adamantyl). (b) Electronic spectra of $MeReO_m(NAr)_n$ (Ar = 2,6-diisopropylphenyl).

the absorbance−time data were analyzed by either of these equations

$$[(\mathbf{1},\mathbf{2a})]_t = [(\mathbf{0},\mathbf{3a})]_0 \times \exp\{-k_{4a}[(\mathbf{3},\mathbf{0})]_{xs}t\} \quad (6)$$

$$\mathrm{Abs}_t = \mathrm{Abs}_e + (\mathrm{Abs}_0 - \mathrm{Abs}_e)\exp(-k_{4a}[(3,0)]_{xs}t) \quad (7)$$

where $[(\mathbf{3},\mathbf{0})]_{xs}$ represents the midpoint concentration during reaction 4a, $[(\mathbf{3},\mathbf{0}]_0 - 1.5[(\mathbf{0},\mathbf{3a})]$. This analysis was checked by using a more elaborate treatment for second-order reversible reactions,[16] but it gave the same results and was not used further.

Reaction 4a was also studied directly by monitoring the absorbance increase at 360 nm under pseudo-first-order conditions with (**3**,**0**) in large excess. The stock solution of (**1**,**2a**) was prepared by mixing 1 equiv of (**3**,**0**) and 2 equiv of (**0**,**3a**). The same second-order rate constant was obtained when the stock solution of (**1**,**2a**) was prepared from the isolated solid, Figure S-1.

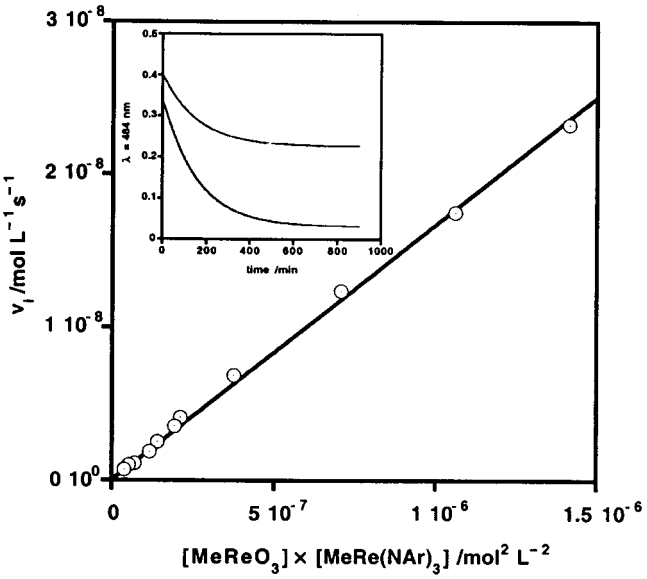

Figure 2. Plot of initial rates for the $MeReO_3$ (**3**,**0**)/$MeRe(NAr)_3$ (**0**,**3b**, Ar = 2,6-diisopropylphenyl) reaction against the product of [**3**,**0**] and [**0**,**3b**]. Conditions: [**3**,**0**] = 0.52−5.0 mM; [**0**,**3b**] = 0.014−0.28 mM; solvent = C_6H_6; temp = 25 °C. The inset shows full kinetic traces of 0.028 and 0.043 mM of **0**,**3b** with 5.0 mM of **3**,**0**.

(b) Reaction 2b. Single-exponential traces were obtained for the reactions of 5.0 mM (**3**,**0**) with 0.028 and 0.043 mM of (**0**,**3b**) by monitoring the disappearance of (**0**,**3b**) at 484 nm, Figure 2. Although the absorbance changes were different for the two kinetic profiles, the observed rate constants were the same regardless of the concentration difference of the limiting reagent. Owing to the slowness of this reaction, thorough kinetic studies were carried out using the initial rate method. The initial rates were linearly proportional to [**3**,**0**] (0.52−5.0 mM) and to [**0**,**3b**] (0.014−0.28 mM). The slope of the plot of initial rates versus the concentration product [**3**,**0**] × [**0**,**3b**], Figure 2, gave $k_{2b} = 0.017(1)$ L mol^{-1} s^{-1}.

(c) Reaction 4b. This reaction was studied directly by mixing the desired concentrations of (**1**,**2b**) and (**3**,**0**). Specifically, the disappearance of 0.024 mM of (**1**,**2b**) was followed at 425 nm as [(**3**,**0**)] changed from 3.0 to 16 mM. Full time-course data to >4 half-times were collected, and $k_{4b} = 0.27(1)$ L mol^{-1} s^{-1} resulted from the pseudo-first-order analysis, Figure 3.

(d) Reaction 3b. ^{1}H NMR spectroscopy was used to obtain the time profiles of the intensities of (**2**,**1b**), (**1**,**2b**), and (**0**,**3b**). An example of this reaction with 11 mM of (**0**,**3b**) and 10 mM of (**2**,**1b**) is given in Figure S-2. A kinetics simulation program, KinSim,[17] was used to analyze the concentration changes of the imidorhenium complexes. A reaction scheme containing reactions 2−4 and the known equilibrium and rate constants were used in the simulation, the only unknown being k_{3b}. The best match between the simulated kinetic profiles and the experimental data was obtained when the forward rate constant $k_{3b} = 0.0024$ L mol^{-1} s^{-1}, Figure S-3.

(e) Reactions 2a and 3a. As mentioned previously, reaction 2a cannot be studied by monitoring the absorbance change of a solution with excess of (**3**,**0**) over (**0**,**3a**). ^{1}H NMR spectroscopy was used to estimate these rate constants when excess (**0**,**3a**) was mixed with (**3**,**0**). Both reactions, 2a and 3a, were detected, particularly when the experiment was carried out at 283 K with millimolar concentrations of (**0**,**3a**) and (**3**,**0**).

Temperature Profiles. The Eyring plots for reactions 4a and 2b are given in Figure 4. Activation parameters were calculated

(16) Espenson, J. H. *Chemical Kinetics and Reaction Mechanisms*, 2nd ed.; McGraw-Hill: New York, 1995.

(17) Barshop, B. A.; Wrenn, C. F.; Frieden, C. *Anal. Biochem.* **1983**, *130*, 134.

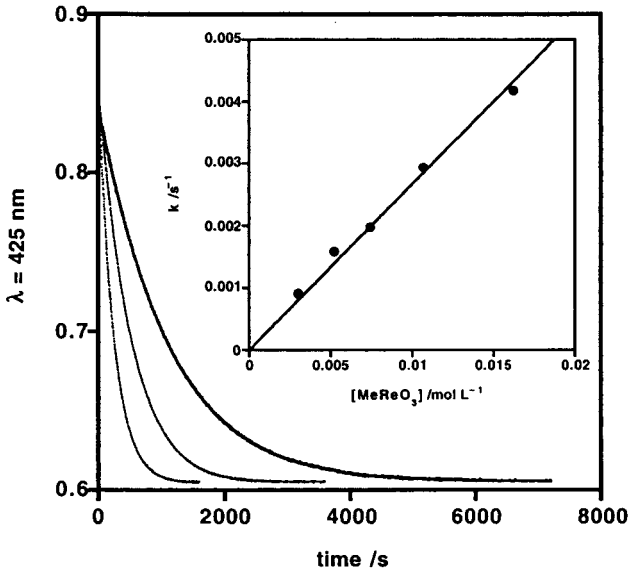

Figure 3. Full kinetic traces for reaction 4b as the [**3**,**0**] increases from 5.2 to 16 mM. The inset shows the plot of pseudo-first-order rate constants for the $MeReO_3$ (**3**,**0**)/$MeReO(NAr)_2$ (**1**,**2b**, Ar = 2,6-diisopropylphenyl) reaction against [**3**,**0**]. Conditions: [**3**,**0**] = 3.0−16 mM; [**1**,**2b**] = 0.024 mM; solvent = C_6H_6; temp = 25 °C.

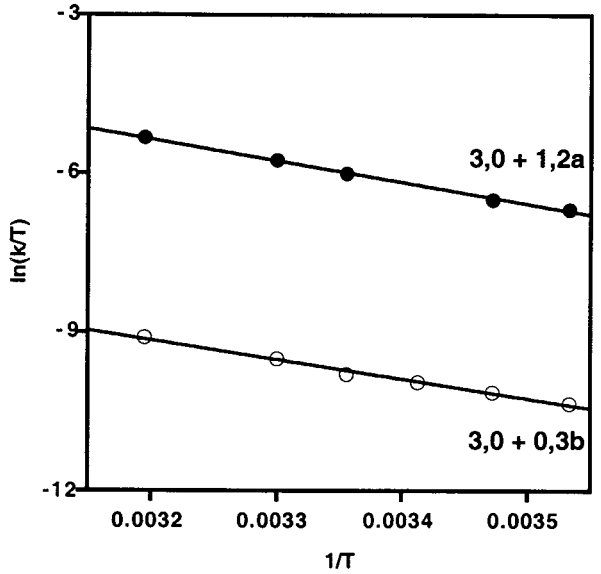

Figure 4. Eyring plots for the reactions of $MeReO_3$ (**3**,**0**)/$MeReO(NAd)_2$ (**1**,**2a**, Ad = 1-adamantyl) (●) and $MeReO_3$ (**3**,**0**)/$MeRe(NAr)_3$ (**0**,**3b**) (○).

over a temperature range 283−313 K from the least-squares fit of values of ln(*k*/T) to 1/*T*, according to the equation

$$\ln\left(\frac{k}{T}\right) = \ln\left(\frac{k_B}{h}\right) + \frac{\Delta S^{\ddagger}}{R} - \frac{\Delta H^{\ddagger}}{RT} \qquad (8)$$

Results

Equilibrium Constants. The ^1H NMR spectrum of a C_6D_6 solution of (**2**,**1b**) showed a mixture containing small amounts of (**3**,**0**) and (**1**,**2b**). The proportions of the three species varied upon addition of more (**3**,**0**) or (**1**,**2b**); however, K_{4b} remained at 84(7). Similarly, $K_{3b} = 22(2)$ was measured by adding different amounts of (**0**,**3b**) into a C_6D_6 solution of (**2**,**1b**). Because the sum of reactions 3b and 4b is 2b, $K_{2b} = 1800(200)$, calculated but not measured directly. As shown in Table 1, in all the cases the equilibrium favors the mixed imido−oxo complexes. The equilibrium constants for the adamantyl series, determined similarly, were slightly larger than those of the corresponding aryl series. Mixed imido−oxo complexes are also favored for the alkylimido system over the arylimido system as observed by Gibson's group. For example, the equilibrium constant toward the mixed compounds is ∼200 for the $(Bu^tO)_2Mo(O)_2/(Bu^tO)_2Mo(N^tBu)_2$ system, but only ∼1 for the $(Bu^tO)_2Mo(O)_2/(Bu^tO)_2Mo(NAr)_2$ system.[18]

The temperature effect on K_{3b} was studied. Over the range 25−50 °C, it decreased slightly, but the change lay within the experimental error. Thus, the enthalpy change is nearly zero, and the driving force for the equilibration reactions is provided by the entropy factor: $\Delta H^{\circ}_{3b} \sim 0$, and $\Delta S^{\circ}_{3b} = 25(2)$ J K^{-1}.

Rate Constants. A summary of rate constants for reactions 2−4 is given in Table 1. These metathesis reactions favor one direction to the extent that the kinetic profiles could be fitted to single-exponential kinetics when one of the reactants was in large excess. Kinetic data collection and analyses were described in detail in the Experimental Section. Most of the rate constants in Table 1 were measured directly or calculated from the known equilibrium constants and directly measured numbers. A few were estimated on the basis of limited data and simulation. It might seem that the kinetics of eq 2b would be complicated in the presence of excess of (**3**,**0**) owing to the subsequent reaction 4b. However, the rate of the disappearance of (**0**,**3b**) in reaction 2b is first-order with respect to [(**3**,**0**)] and [(**0**,**3b**)], and reaction 4b is more than 10 times faster than reaction 2b. This clearly suggests that the rate-controlling step of the reaction between (**0**,**3b**) and a large excess of (**3**,**0**) is reaction 2b. Although reactions 2b and 4b were clean, the kinetic traces of reaction 3b consisted of two stages. The first involves reaction 2b between (**0**,**3b**) and (**3**,**0**), followed by the slower reaction 3b between (**2**,**1b**) and (**0**,**3b**). The small amount of (**3**,**0**) in the stock solution of (**2**,**1b**) results from the disproportionation of (**2**,**1b**), the reverse of reaction 2b. This set of reactions, as stated, was modeled successfully by the KinSim program, Figure S-3. The curvature of the initial part for [(**0**,**3b**)] is sensitive to $[(\mathbf{3},\mathbf{0})]_0$, a value that is not certain.

Identical (within experimental error) rate constants and activation parameters were obtained for the reactions prepared with the combinations (**3**,**0**) + (**0**,**3a**) and (**3**,**0**) + (**1**,**2a**). Careful NMR kinetic analysis at low temperature suggested that reaction 2a was faster than 4a and the rate constants obtained from spectrophotometric studies are for reaction 4a, regardless of whether the reaction was initiated with (**0**,**3a**) or (**1**,**2a**).

Activation Parameters. Kinetic data were collected over 10−40 °C. The Eyring plots, Figure 4, were given for the reactions 2b and 4a. The activation entropies are $\Delta S^{\ddagger}_{4a} = -134(4)$ J K^{-1} and $\Delta S^{\ddagger}_{2b} = -175(4)$ J K^{-1}; the activation enthalpies are $\Delta H^{\ddagger}_{2b} = 31(1)$ kJ and $\Delta H^{\ddagger}_{4a} = 34(1)$ kJ. The

(18) The cited value in ref 14 has been corrected to this value [Gibson, V. C. Private communication].

Scheme 1

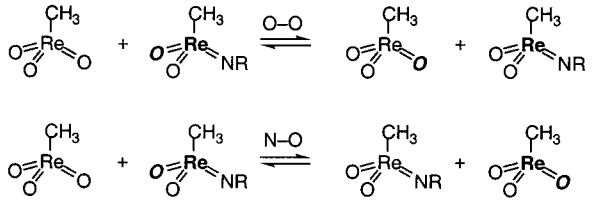

Table 2. Activation Parameters for Intermetal Imido−Oxo Exchange Reactions

reaction	$\Delta S^{\ddagger}$/J mol^{-1} K^{-1}	$\Delta H^{\ddagger}$/kJ mol^{-1}
4a	−134 (4)	34 (1)
2b	−175 (4)	31 (1)
4b	−158 (2)	29.2 (0.6)
5[a]	− 79 (8)	86 (2)

[a] Reaction 5 is $MoO_2(O^tBu)_2 + Mo(NAr)_2(O^tBu)_2 \rightleftarrows 2MoO(NAr)(O^tBu)_2$.

activation parameters for reaction 4b and for the $MoO_2(O^tBu)_2/Mo(NAr)_2(O^tBu)_2$ reaction[14] are also given in Table 2.

Other Metathesis Reactions. Attempts to prepare mixed imido complexes, $MeRe(NAd)_n(NAr)_{3-n}$, from the reaction of (**0**,**3a**) and (**0**,**3b**) failed. The ^{1}H NMR spectrum of the solution containing 20 mM of (**0**,**3a**) and 20 mM of (**0**,**3b**) in C_6D_6 remained the same at room temperature for 72 h. The reaction of $MeRe^{17}O_3$ and (**2**,**1b**) in C_6D_6 took place as monitored by an ^{17}O NMR technique. The incorporation of ^{17}O into (**2**,**1b**) was confirmed by the NMR spectrum. However, the observation of $MeRe^{17}O(NAr)_2$ from the $MeRe^{17}O_3/MeReO_2(NAr)$ reaction cannot be used to differentiate the two possible scenarios shown in Scheme 1. The $^3J_{17O-H}$ coupling was observed neither for $MeRe^{17}O_3$ nor $MeRe^{17}O(NAr)_2$.

The reactions of 7.4 mM (**3**,**0**) and 0.095 mM (**0**,**3b**) in the presence of acid and bases were studied spectrophotometrically. Nearly identical kinetic profiles were observed at 484 nm for the reactions with 0, 4.4, and 8.8 mM of 2,6-diisopropylaniline. When 4-^{t}Bu-pyridine was used, the initial rates decreased as [4-^{t}Bu-pyridine] increased from 5.6 to 11 mM. The hydrolyses of (**1**,**2b**) and (**0**,**3b**) are much slower than those exchange reactions with (**3**,**0**).[2] Because 2,6-diisopropylaniline, a hydrolysis product, had shown no effect on the oxo/imido exchange, the effect of water was not pursued here. Trifluoroacetic acid did affect the exchange reaction between (**3**,**0**) and (**0**,**3b**); however, a similar effect was observed even in the absence of (**3**,**0**). Preliminary results showed that CF_3COOH accelerated the hydrolysis of (**0**,**3**).

Discussion

Metathesis Mechanism. A mechanism involving a 4-center transition state for reactions of metal−ligand multiple bonds and unsaturated reagents is well documented.[19] An analogous mechanism, supported by a large negative activation entropy, has been proposed for imido and oxo intermetal exchange reactions between $(Bu^tO)_2Mo(O)_2$ and $(Bu^tO)_2Mo(NAr)_2$.[14] The large negative activation entropies of the reactions in Table 2 are consistent with an ordered transition state.

(19) Nugent, W. A.; Mayer, J. M. *Metal−Ligand Multiple Bonds*; Wiley-Interscience: New York, 1988.

Scheme 2

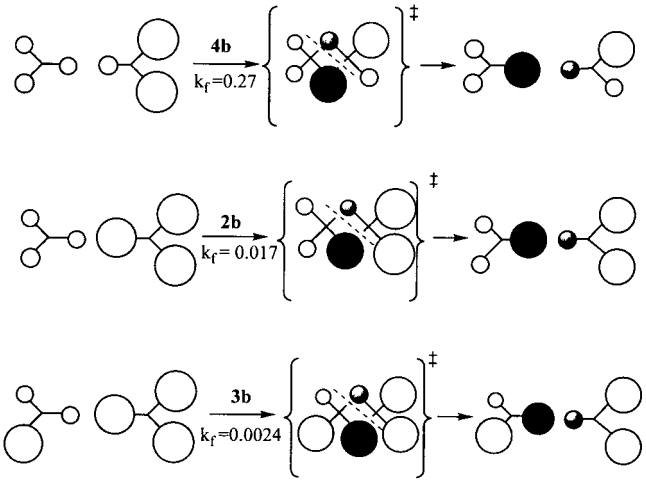

As mentioned previously for reactions 2−4, a net reaction occurs only when the transition state contains one imido and one oxo bridge. If the two bridging groups are the same, self-exchange reactions may take place. For example, reaction between (**3**,**0**) and (**1**,**2**) will lead to a net change when the transition state contains mixed bridges, eq 4, whereas self-exchange will result with the isomeric transition state comprising two oxo bridges. Not all mixed-bridged intermediates will lead to a net reaction. For example, reactions shown in Scheme 1 result from both oxo−oxo and oxo−imido bridged intermediates. Double isotopic labeling would be required to elucidate the mechanisms of these reactions.

Although 2,6-diisopropylaniline has shown no effect on the oxo/imido exchange reaction, 4-^{t}Bu-pyridine clearly slows down the process. There is no observable interaction between ligands, such as phosphine and pyridine, and (**0**,**3b**). However, it is known that sterically less bulky pyridines will bind to (**3**,**0**).[20] The strong interaction between 4-^{t}Bu-pyridine and (**0**,**3b**) ($K_{eq} > 500$ in C_6H_6) will significantly reduce the amount of free (**3**,**0**) in solution.[21] The inhibition by 4-^{t}Bu-pyridine and the lack of effect of 2,6-diisopropylaniline result from their different binding ability toward (**3**,**0**). Most recently, Gibson and co-workers have discovered that Brønsted acids catalyze the intermetal−ligand exchange reactions.[22] Preliminary results for the rhenium(VII) system show that the protic acid CF_3COOH accelerates the hydrolysis of (**0**,**3b**). Further experiments would be needed to distinguish hydrolysis from exchange and to elucidate the role of acid on the imido/oxo exchange reactions.

Reactivity. Table 1 shows that the rate constants decrease as the total number of 2,6-diisopropylphenylimido ligands increases. This suggests that significant steric crowding in the transition state raises the activation barrier. The diagram in Scheme 2, which presents the steric conflict, shows how that can come about. Steric effects on the kinetics of oxo−imido exchange in Mo compounds have been reported previously.[14] Steric effects are also the likely cause of the lack of reaction between (**0**,**3a**) and (**0**,**3b**).

(20) Wang, W.-D.; Espenson, J. H. *J. Am. Chem. Soc.* **1998**, *120*, 11335.
(21) Wang, W.-D.; Espenson, J. H. Unpublished result.
(22) Blackmore, I. J.; Gibson, V. C.; Graham, A. J.; Jolly, M.; Marshall, E. L.; Ward, B. P. *J. Chem. Soc., Dalton Trans.* **2001**, 3242.

Scheme 3

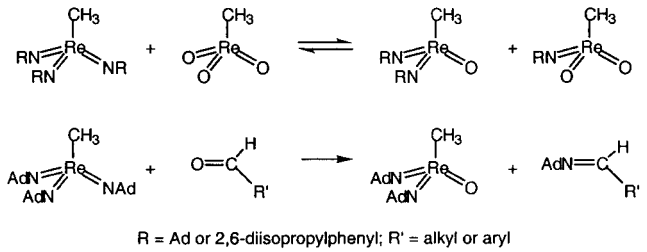

Table 3. Comparison of Rate Constants (L mol^{-1} s^{-1}) for Metathesis Reactions with $CH_3Re(NAd)_3$ (**0**,**3a**) and $CH_3Re(NAr)_3$ (**0**,**3b**)

	$CH_3(O)_2Re{=}O$	*n*-$C_3H_7HC{=}O$	4-$NO_2C_6H_4HC{=}O$
$CH_3Re(NAd)_3$	>100	0.032	0.0007
$CH_3Re(NAr)_3$	0.017	NA	NR

The reactivities for oxo exchange of (**3**,**0**) as compared to aldehydes are noteworthy. Only the adamantylimido compounds react with aldehydes to produce oxo−imido complexes and organic imines.[1] Aldehyde exchange is restricted to the alkylimido rhenium compounds, although both alkylimido and arylimido rhenium complexes undergo oxo exchange with (**3**,**0**), Scheme 3. This difference possibly arises from the high reactivity of the Re=O moiety in (**3**,**0**), compared with that of the C=O group in aldehydes. Comparison of the reactivity for the Re=O of (**3**,**0**) versus the C=O of aldehydes is given in Table 3.

Thermodynamic Considerations. The entropic effect probably plays an important role in the imido−oxo exchange reactions ($\Delta S_{3b}° = 25(2)$ J K^{-1} and $\Delta H_{3b}° \sim 0$). A purely statistical analysis[23] gives $K_2 = 9$, $K_3 = 3$, and $K_4 = 3$, much smaller than the experimental values, Table 1. Different steric demands of imido and oxo ligands are neglected in the statistical estimate. When the bulky imido ligands reside on one rhenium center, free rotations of the $N-C_{Ar}$ bonds and the *i*Pr groups are possibly restricted. The large equilibrium constants for reaction 2 likely result from the release of the steric crowding around (**0**,**3**). It is interesting to note that the equilibria of imide−imide metathesis reactions studied by Gibson[14] and Meyer[11] also favor the mixed ligand complexes. In the imide−imide case, the steric factor may not be as significant as in the oxo−imido system because the difference between the relative steric demand of the two imido groups, N^{t}Bu and NAr, is less pronounced than that between oxo and bulky imido ligands. The analogous imine−imine exchange reactions have an equilibrium constant that is nearly unity.[1,11] This preference for mixed-ligand species has found synthetic utility for transition metal imido−oxo complexes. For example, the metathesis reaction between (**3**,**0**) and (**1**,**2b**) was used to obtain (**2**,**1b**), which was fully characterized.[3] A mixed imido−oxo complex, $MoCl_2$(Nmes)(O)(dme) (mes = 2,4,6-trimethylphenyl; dme = 1,2-dimethoxyethane), was prepared in high yield from $MoCl_2$(Nmes)$_2$(dme) and $MoCl_2O_2$(dme).[24] Another interesting reaction affords $Os(NAr)_2O_2$ and $(Bu^tO)_2MoO_2$ from OsO_4 and $(Bu^tO)_2Mo(NAr)_2$.[25] Both enthalpic and entropic factors may have played key roles in this clean imido−oxo exchange reaction between two different metal centers.

Acknowledgment. This research was supported by a grant from the National Science Foundation. Some experiments were conducted with the use of the facilities of the Ames Laboratory. We are grateful to Dr. A. P. Sattelberger of Los Alamos National Laboratory for supplying $H_2{}^{17}O$.

Supporting Information Available: Tables for equilibrium constant measurements and exchange processes that do not lead to net change and figures for kinetics, NMR spectra, and simulation (6 pages). This material is available free of charge via the Internet at http://pubs.acs.org.

IC011070P

(23) Shriver, D. F.; Atkins, P. W.; Langford, C. H. *Inorganic Chemistry*; W. H. Freeman and Company: New York, 1990.

(24) Galindo, A.; Montilla, F.; Pastor, A.; Carmona, E. *Inorg. Chem.* **1997**, *36*, 2379.

(25) Wolf, J. R.; Bazan, G. C.; Schrock, R. R. *Inorg. Chem.* **1993**, *32*, 4155.